DIVAID: Automatic Division of Bi-Atrial Geometries Into Clinically Important Regions

Christian Goetz[1,2], Patricia Martínez Díaz[2], Till Althoff[3], Constanze Schmidt[1], Axel Loewe[2]

[1] Department of Cardiology, Heidelberg University Hospital, Heidelberg, Germany
[2] Institute of Biomedical Engineering, Karlsruhe Institute of Technology (KIT), Karlsruhe, Germany
[3] Department of Cardiology, Clínic - University Hospital Barcelona, Barcelona, Spain

Abstract

Recent technological advances in cardiac imaging, e.g. cardiac computed tomography (CT), magnetic resonance imaging (MRI) and electroanatomical mapping (EAM) allow detailed analyses of cardiac morphology and function. However, to perform regional quantitative intra- and inter-individual, as well as cross-modality comparisons, a standard for the regionalization of the heart is required. We developed a 15-region bi-atrial model based on anatomical, electrophysiological and clinical considerations. Moreover, we devised a pipeline (DIVAID) to automatically divide any bi-atrial geometry according to our proposed definitions. The automatic division results were compared to blinded manual expert regionalizations in 20 bi-atrial geometries from multiple acquisition modalities. The mean regional overlap (Dice score) between both division results across all geometries for both atria combined was 0.92. The mean Euclidean distance between regional boundaries derived from either manual or automatic division in both atria was 1.70 mm. Given the high concordance between both division results, this algorithm enables standardized, consistent, reproducible and operator-independent regional quantitative comparisons of the atria between multiple modalities, patients and centers, which may facilitate cardiac research towards personalized treatment approaches.

1. Introduction

Cardiovascular diseases are the leading cause of death globally. Recent technological advances in multiple acquisition modalities, such as CT, MRI and EAM allow more detailed analyses of cardiac morphology and function. However, to perform regional quantitative inter- and intra-individual, as well as cross-modality comparisons, a standard nomenclature for the regionalization of the heart is required. While a standardized regionalization of the left ventricle (AHA 17-segment model) has been established, there is currently no consensus regarding the regionalization of the atria [1]. To date, atrial regionalizations previously described in the literature were not intended for universal applicability; instead, they were mostly tailored to meet the specific requirements of particular analyses [2–6]. Here, we present an algorithm to consistently and robustly divide any bi-atrial geometry into standardized atrial regions which are based on anatomical, electrophysiological and clinical considerations. This allows for reproducible, operator-independent regional quantitative comparison between multiple modalities, individuals and institutions.

2. Methods

In a collaborative effort within the European PersonalizeAF consortium involving cardiologists, electrophysiologists, anatomists, as well as experts in cardiac imaging and computational modeling, a regionalization standard based on a 15-region bi-atrial model was formulated. We conducted a literature research on previously proposed regional definitions and followed the criteria used for the development of the AHA 17-segments ventricular model. Thus, we adopted widely accepted definitions of regions and based our regional definitions on anatomical landmarks while considering the anatomical variety of the atria. The proposed standardized regionalization can be used for current imaging acquisition modalities by providing adequate sampling of the regions without exceeding resolution limits of any modality. The regional boundaries are based on the shortest geodesic paths between two precisely defined points using anatomical orientations, e.g. between the most superior aspect of the left superior pulmonary vein (LSPV) ostium and most superior aspect of the right superior pulmonary vein (RSPV) ostium. A list with definitions of all reference points is shown in Table 1. For the left atrium (LA), the proposed regions comprise the left venoatrial junction, right venoatrial junction, posterior wall, anterior wall, left atrial appendage (LAA), lateral wall, inferior wall and septal wall, as illustrated in Figure 1. The regions in the right atrium (RA) include the

 Page 1 ISSN: 2325-887X DOI: 10.22489/CinC.2024.316

Table 1: Definition of reference points in the LA (top section) and RA (bottom section). PV = pulmonary vein, MV = mitral valve, TV = tricuspid valve, SVC = superior vena cava, IVC = inferior vena cava, CS = coronary sinus, LAA = left atrial appendage, RAA = right atrial appendage, RS = right superior, LS = left superior, RI = right inferior, LI = left inferior

Point	Definition
A	most superior aspect of the RSPV ostium
B	most superior aspect of the LSPV ostium
C	most inferior aspect of the LIPV ostium
D	most inferior aspect of the RIPV ostium
E	9 o'clock position on the MV
F	1 o'clock position on the MV
G	closest point to B on the LAA ostium
H	closest point to F on the LAA ostium
I	closest point to C on the LAA ostium
J	4 o'clock position on the MV
K	7 o'clock position on the MV
L	most anterior aspect of the SVC ostium
M	most septal aspect of the SVC ostium
N	most lateral aspect of the SVC ostium
O	most septal aspect of the IVC ostium
P	most lateral aspect of the IVC ostium
Q	1 o'clock position on the TV
R	5 o'clock positoin on the TV
S	8 o'clock position on the TV
T	11 o'clock position on the TV
U	maximum curvature between RAA and anterior wall
V	most lateral aspect in anterior oblique view horizontally to U
W	point at 2/3 of the shortest geodesic path from P to S
X	most inferior aspect of the CS ostium

septal wall, posterior venous wall, right atrial appendage (RAA), lateral vestibule, anterior wall, cavotricuspid isthmus (CTI) and Koch's triangle.

To provide a tool realizing the regionalization and to enable accurate operator-independent regional quantitative comparisons, we developed a robust and consistent atrial division pipeline (DIVAID, gitlab.kit.edu/kit/ibt-public/divaid [7]) which automatically divides any bi-atrial geometry into the proposed regions. The division pipeline encompasses 3 steps: standardization, ring extraction and division.

The algorithm is capable of processing both mono-atrial (LA or RA) and bi-atrial geometries with a surface mesh in VTK format, provided that the mitral valve (MV) and tricuspid valve (TV) ostia are open. First, the input geometry is standardized to reduce the influence of model- and geometry-related variations on the division. The surface mesh is resampled with a uniform edge length of 1 mm using explicit isotropic remeshing [8]. Additionally, the veins are clipped semi-automatically by interactively selecting seed nodes on the tips or orifices of the veins and by computing centerlines from the seed nodes to the barycenter of the MV or TV, respectively [9]. The point on the centerline at which the enclosed cross-sectional area exhibits an abrupt increase marks the location where a vein transitions into the atrial body [10]. The same procedure is applied to temporarily clip the LAA.

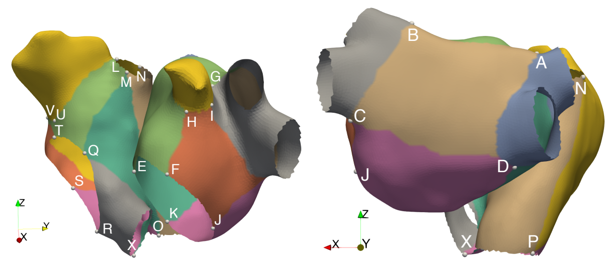

(a) Superolateral view (b) Posterior view

Figure 1: Overview of all points and regions. LA / RA: ■ Left venoatrial junction / Koch's triangle, ■ right venoatrial junction, ■ posterior wall, ■ anterior wall, ■ LAA / RAA, ■ lateral wall / lateral vestibule, ■ inferior wall / cavotricuspid isthmus, ■ septal wall

Second, the ostia are automatically extracted and annotated [11]. This process enables annotations of LA ostia with 3, 4 or 5 PVs.

Third, the geometries are divided according to the proposed definitions. The previously defined points are derived by using the extracted annotated ostia and the attitudinal anatomical orientation of the atria, i.e., the body coordinate system. Further details are provided in the code documentation [7]. The regional boundaries are determined by computing the shortest geodesic paths between two corresponding points.

Regarding the LA, the points on the PV ostia are defined as either the most superior or most inferior aspects. Thus, the nodes on the PV ostia exhibiting the highest or lowest attitudinal z-value are identified, respectively. For the MV, a clock model is introduced with the viewpoint from the left ventricle towards the roof at which 12 o'clock marks the projection of the z-axis on the MV annulus originating from the MV center. Points E, F, J and K are obtained by fitting a plane to the MV using Singular Value Decomposition and subsequently rotating the projected z-axis by the corresponding angle employing Rodrigues' rotation formula. Points G, H and J are derived by calculating the distances between all points on the LAA boundary and either point B, F or C, respectively, followed by extraction of the points with the smallest distances.

For the RA, points L-P are obtained accordingly to points A-D. Similarly to the LA, a clock model is introduced for the TV. The z-axis is projected on the TV annulus originating from the TV center to obtain the 12 o'clock position. Points Q-T are derived accordingly to the LA by employing Rodrigues' rotation formula. Due to the great variability of the RAA and the typically non-smooth surface mesh, the automatic extraction of the point with the maximum curvature between the RAA and the anterior wall is challenging. For details on the identification of point U and V, please refer to the code documentation. Point W is defined as the node at 2/3 of the shortest geodesic path between point P and point S. Point X is derived accordingly to points A-D.

The corresponding regions are obtained through iterative removal of the boundaries defining each region from the mesh, followed by the extraction of the largest connected region. The nodes comprising the respective region are then identified by subtracting the obtained nodes from all nodes of the mesh. The output file includes all data (e.g. voltages or intensities) from the input file complemented by an array with region tags for each node.

To validate the accuracy of the automatic division, we compared the division results to blinded manual expert annotations in 20 bi-atrial geometries from multiple acquisition modalities (CT and MRI). For quantitative comparisons between both division results, we used the identical mesh with clipped veins, i.e. the result of step 2 from DIVAID, for the manual division. For the manual regionalization, the points were placed interactively on the mesh and the regional boundaries were obtained as the shortest geodesic paths between the manually selected points. The regional overlap between the division results from the automatic and manual division methods was evaluated using the Dice score. Additionally, we computed the mean Euclidean distance between the regional boundaries derived manually and automatically. For each node on the manually derived boundary, the closest node on the automatically derived boundary was identified and the Euclidean distance was calculated.

3. Results

All 20 bi-atrial geometries were successfully divided into the proposed regions for both, the manual and automatic method. The mean regional overlap (Dice score) between both division results across all geometries for both atria combined was 0.92 (see Figure 2a-b). In the LA, the mean Dice score was 0.95 with the lowest mean regional overlap in the inferior wall (0.92) and the highest mean regional overlap in the right venoatrial junction (0.99). In the RA, the mean Dice score was 0.88 with the lowest mean regional overlap observed in the lateral vestibule (0.75) and the highest mean regional overlap found in Koch's triangle (0.94).

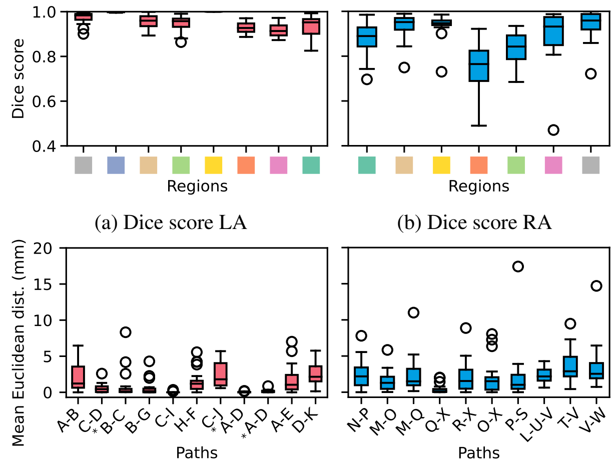

(a) Dice score LA (b) Dice score RA

(c) Mean Euclidean distance LA (d) Mean Euclidean distance RA

Figure 2: Validation of the accuracy of the automatic regionalization through comparison with manual expert annotations. (a-b) Dice scores for each region in the LA and RA. (c-d) Mean Euclidean distance per path in the LA and RA. * denotes the superior path, while $_*$ indicates the inferior path.

The mean Euclidean distance between regional boundaries obtained from either manual or automatic division across all geometries for both atria combined was 1.70 mm (see Figure 2c-d). Note that the LAA was excluded from this analysis as its regional boundary has already been defined during the vein clipping procedure. In the LA, the mean Euclidean distance between regional boundaries from both division results was 1.16 mm. The paths from the most inferior aspect of the LIPV ostium (point C) to the closest node on the LAA ostium (point I) showed the smallest mean Euclidean distance with 0.02 mm, while the paths from the most inferior aspect of the RIPV ostium (point D) to the 7 o'clock position on the MV (point K) showed the highest mean Euclidean distance with 2.62 mm. Regarding the RA, the mean Euclidean distance between regional boundaries from both division results was 2.25 mm. The paths from the 1 o'clock position on the TV (point Q) to the most inferior aspect of the CS (point X) exhibited the smallest mean Euclidean distance with 0.42 mm and the highest mean Euclidean distance was observed for the paths from the 11 o'clock position on the TV (point T) to the most lateral aspect at the transition between the RAA and the anterior wall (point V) with 3.64 mm.

Figure 3 illustrates an example of the comparison between manual and automatic division results. The mean Euclidean distance between the paths connecting the most

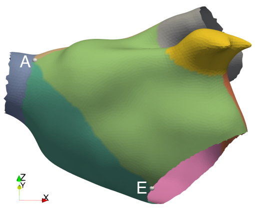

(a) Automatic division

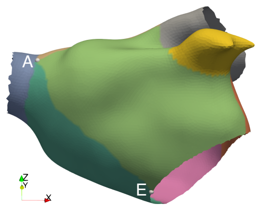

(b) Manual division

Figure 3: Comparison of the division results.

superior aspect of the RSPV (point A) and the 9 o'clock position on the MV (point E) was 2.16 mm. The regional overlap of the anterior wall was 0.96. The mean Euclidean distance between the 1 o'clock position on the MV (point F) and the closest node on the LAA ostium to point F (point H) was 1.27 mm.

The mean duration for automatically dividing an atrium (LA or RA) was 1.1 s, while the mean duration for the manual division was 3 min per atrium.

4. Discussion

The higher agreement between manual and automatic regionalization in the LA compared to the RA can be explained by the symmetric shape of the LA and the presence of multiple significant landmarks. In contrast, the RA shows a higher anatomical variability and asymmetry with fewer prominent landmarks compared to the LA. At the transition between the RAA and the anterior wall, no significant landmarks can be used to accurately define the points U and V, which may explain the differences between the manual and automatic divisions. Moreover, the RAA shows a high anatomical variability further increasing the challenge of accurate annotations in this area.

As illustrated in Figure 3, both division results show a high visual concordance. The mean Euclidean distance of 2.16 mm between the path from the most superior aspect of the RSPV (point A) and the 9 o'clock position on the MV (point E), obtained through either manual or automatic division, suggests that a mean Euclidean distance of 1.70 mm is barely perceptible visually and does not significantly impact the overall division result. Moreover, regarding the resolution of the acquired MRI images (voxel size of 1.25 x 1.25 x 2.4 mm), this implies a deviation of less than two voxels.

In conclusion, this open source algorithm enables standardized, consistent, reproducible and operator-independent regional quantitative comparisons of the atria between multiple modalities, patients and centers, which may facilitate cardiac research towards personalized treatment approaches.

Author Statement

This project has received funding from the European Union's Horizon 2020 research and innovation programme under the Marie Skłodowska-Curie grant agreement No 860974. This work was supported by the Leibniz Science-Campus "Digital Transformation of Research" with funds from the programme "Strategic Networking in the Leibniz Association".

References

[1] Cerqueira MD, Weissman NJ, Dilsizian V, et al. Standardized myocardial segmentation and nomenclature for tomographic imaging of the heart. Circ 2002;105(4):539–542.

[2] Haissaguerre M, Hocini M, Denis A, et al. Driver domains in persistent atrial fibrillation. Circ 2014;130:530–538.

[3] Benito EM, Cabanelas N, Nuñez-Garcia M, et al. Preferential regional distribution of atrial fibrosis in posterior wall around left inferior pulmonary vein as identified by LGE-MRI in patients with atrial fibrillation. Europace 2018; 20(12):1959–1965.

[4] Chen Y, Ban J, Park Y, et al. The spatial distribution of atrial fibrillation termination sites in the right atrium during complex fractionated atrial electrograms-guided ablation in patients with persistent atrial fibrillation. J Cardiovasc Electrophysiol 2013;24(9):949–957.

[5] Nairn D, Eichenlaub M, Müller-Edenborn B, et al. Differences in atrial substrate localization using late gadolinium enhancement-magnetic resonance imaging, electrogram voltage, and conduction velocity. Europace 2023; 25:euad278.

[6] Williams SE, Tobon-Gomez C, Zuluaga MA, et al. Standardized unfold mapping: a technique to permit left atrial regional data display and analysis. J Intervent Cardiac Electrophysiol 2017;50(1):125–131.

[7] Goetz C, Loewe A, Martínez Díaz P. DIVAID (v1.1), 2024. URL `https://doi.org/10.35097/vrt7udc8uyfej20a`.

[8] Muntoni A, Cignoni P. PyMeshLab, 2021. URL `http://doi.org/10.5281/zenodo.4438750`.

[9] Izzo R, Steinman D, Manini S, Antiga L. The vascular modeling toolkit: A python library for the analysis of tubular structures in medical images. JOSS 2018;3(25):745.

[10] Nunez Garcia M, Bernardino G, Alarcon F, et al. Fast quasi-conformal regional flattening of the left atrium. IEEE TVCG 2020;26(8):2591–2602.

[11] Azzolin L, Eichenlaub M, Nagel C, et al. AugmentA: Patient-specific augmented atrial model generation tool. Comput Med Imaging Graph 2023;108:102265.

Address for correspondence:

Christian Goetz, christian.goetz@partner.kit.edu
Department of Cardiology, Heidelberg University Hospital,
Im Neuenheimer Feld 410, 69115 Heidelberg, Germany